

Quark matter and the astrophysics of neutron stars

M Prakash

Department of Physics & Astronomy, Ohio University, Athens, OH 45701, USA

E-mail: prakash@harsha.phy.ohiou.edu

Abstract. Some of the means through which the possible presence of nearly deconfined quarks in neutron stars can be detected by astrophysical observations of neutron stars from their birth to old age are highlighted.

1. Introduction

Utilizing the asymptotic freedom of QCD, Collins and Perry [1] first noted that the dense cores of neutron stars may consist of deconfined quarks instead of hadrons. The crucial question is whether observations of neutron stars from their birth to death through neutrino, photon and gravity-wave emissions can unequivocally reveal the presence of nearly deconfined quarks instead of other possibilities such as only nucleons or other exotica such as strangeness-bearing hyperons or Bose (pion and kaon) condensates.

2. Neutrino signals during the birth of a neutron star

The birth of a neutron star is heralded by the arrival of neutrinos on earth as confirmed by IMB and Kamiokande neutrino detectors in the case of supernova SN 1987A. Nearly all of the gravitational binding energy (of order 300 bethes, where 1 bethe $\equiv 10^{51}$ erg) released in the progenitor star's white dwarf-like core is carried off by neutrinos and antineutrinos of all flavors in roughly equal proportions. The remarkable fact that the weakly interacting neutrinos are trapped in matter prior to their release as a burst is due to their short mean free paths in matter, $\lambda \approx (\sigma n)^{-1} \approx 10$ cm, (here $\sigma \approx 10^{-40}$ cm² is the neutrino-matter cross section and $n \approx 2$ to $3 n_s$, where $n_s \simeq 0.16$ fm⁻³ is the reference nuclear equilibrium density), which is much less than the proto-neutron star radius, which exceeds 20 km. Should a core-collapse supernova occur in their lifetimes, current neutrino detectors, such as SK, SNO, LVD's, AMANDA, etc., offer a great opportunity for understanding a proto-neutron star's birth and propagation of neutrinos in dense matter insofar as they can detect tens of thousands of neutrinos in contrast to the tens of neutrinos detected by IMB and Kamiokande.

The appearance of quarks inside a neutron star leads to a decrease in the maximum mass that matter can support, implying metastability of the star. This would occur if the proto-neutron star's mass, which must be less than the maximum mass of the

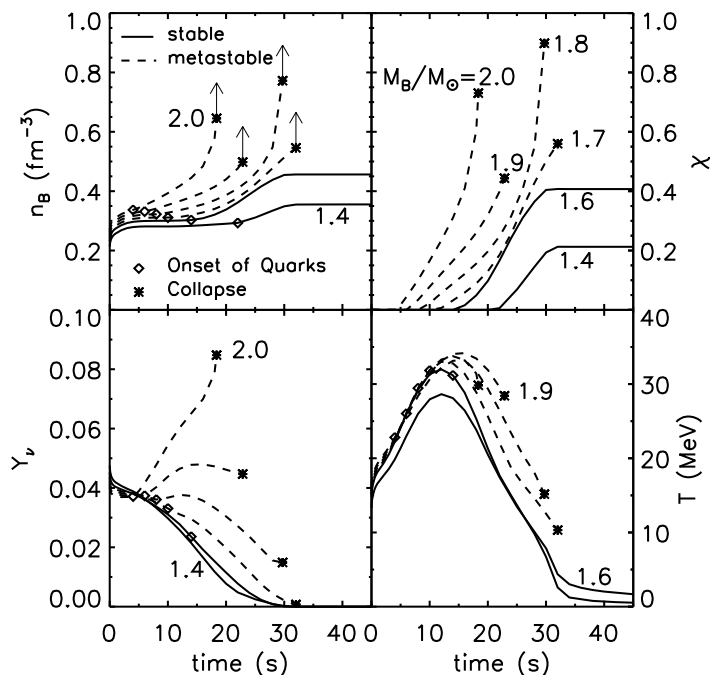


Figure 1. Evolutions of the central baryon density n_B , ν concentration Y_ν , quark volume fraction χ and temperature T for different baryon masses M_B . Solid lines show stable stars whereas dashed lines showing stars with larger masses are metastable. Diamonds indicate when quarks appear at the star’s center, and asterisks denote when metastable stars become gravitationally unstable. Figure after Ref. [2]

hot, lepton-rich matter is greater than the maximum mass of hot, lepton-poor matter. For matter with nucleons only, such a metastability is denied (see, e.g., [3]). Figure 1 shows the evolution of some thermodynamic quantities at the center of stars of various fixed baryonic masses. With the equation of state used (see [2] for details), stars with $M_B \lesssim 1.1 M_\odot$ do not contain quarks and those with $M_B \sim 1.7 M_\odot$ are metastable. The subsequent collapse to a black hole could be observed as a cessation in the neutrino signals well above the sensitivity limits of the current detectors (Figure 2).

3. Photon signals during the thermal evolution of a neutron star

Multiwavelength photon observations of neutron stars, the bread and butter affair of astronomy, has yielded estimates of the surface temperatures and ages of several neutron stars (Fig. 3). As neutron stars cool principally through neutrino emission from their cores, the possibility exists that the interior composition can be determined. The star continuously emits photons, dominantly in x-rays, with an effective temperature T_{eff} that tracks the interior temperature but that is smaller by a factor ~ 100 . The dominant neutrino cooling reactions are of a general type, known as Urca processes [4], in which thermally excited particles undergo beta and inverse-beta decays. Each

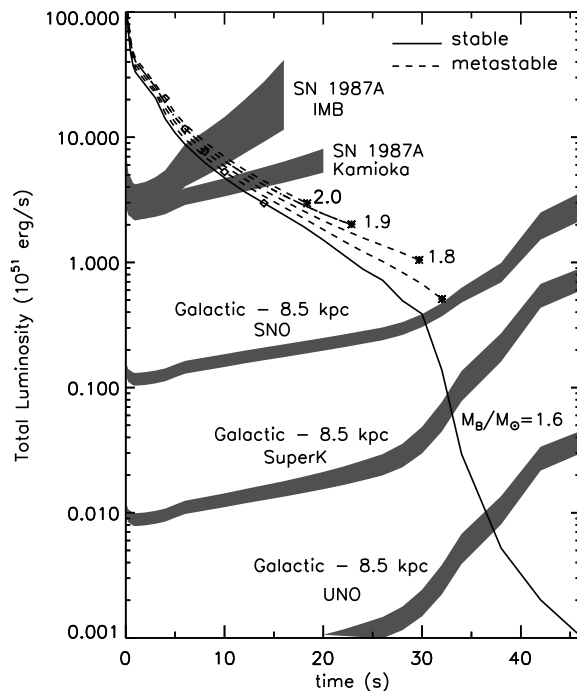


Figure 2. The evolution of the total neutrino luminosity for stars of indicated baryon masses. Shaded bands illustrate the limiting luminosities corresponding to a count rate of 0.2 Hz in all detectors assuming 50 kpc for IMB and Kamioka, 8.5 kpc for SNO, SuperK, and UNO. Shaded regions represent uncertainties in the average neutrino energy from the use of a diffusion scheme for neutrino transport in matter. Figure after Ref. [2].

reaction produces a neutrino or anti-neutrino, and thermal energy is thus continuously lost. Depending upon the proton-fraction of matter, which in turn depends on the nature of strong interactions at high density, direct Urca processes involving nucleons, hyperons or quarks lead to enhanced cooling compared to modified Urca processes in which an additional particle is required to conserve momentum. However, effects of superfluidity abates cooling as sufficient thermal energy is required to break paired fermions. In addition, the poorly known envelope composition also plays a role in the inferred surface temperature (Fig. 3). The multitude of high density phases, cooling mechanisms, effects of superfluidity, and unknown envelope composition have thus far prevented definitive conclusions to be drawn (see, e.g., [5]).

4. Measured masses and their implications

Several recent observations of neutron stars have direct bearing on the determination of the maximum mass. The most accurately measured masses are from timing observations of the radio binary pulsars. As shown in Fig. 4, which is compilation of the measured neutron star masses as of November 2006, observations include pulsars orbiting another

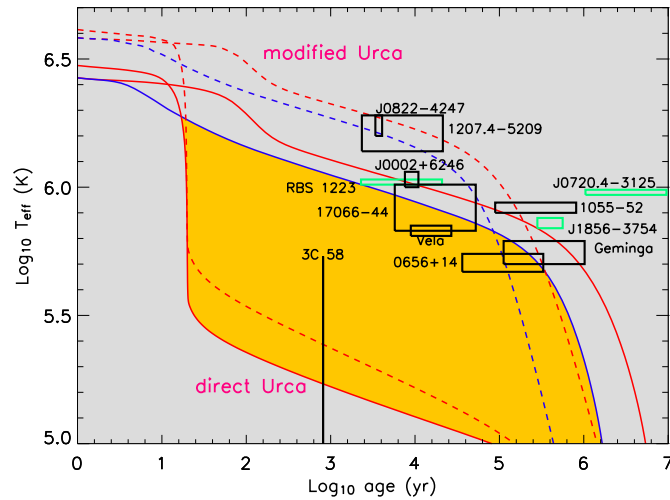


Figure 3. Observational estimates of neutron star temperatures and ages together with theoretical cooling simulations for $M = 1.4 M_{\odot}$. Models and data are described in [6]. Orange error boxes (see online) indicate sources from which both X-ray and optical emissions have been observed. Simulations are for models with Fe or H envelopes, with and without the effects of superfluidity, and allowing or forbidding direct Urca processes. Models forbidding direct Urca processes are relatively independent of M and superfluid properties. Trajectories for models with enhanced cooling (direct Urca processes) and superfluidity lie within the yellow region, the exact location depending upon M as well as superfluid and Urca properties. Figure adapted from Ref. [7].

neutron star, a white dwarf or a main-sequence star.

One significant development concerns mass determinations in binaries with white dwarf companions, which show a broader range of neutron star masses than binary neutron star pulsars. Perhaps a rather narrow set of evolutionary circumstances conspire to form double neutron star binaries, leading to a restricted range of neutron star masses [9]. This restriction is likely relaxed for other neutron star binaries. A few of the white dwarf binaries may contain neutron stars larger than the canonical $1.4 M_{\odot}$ value, including the intriguing case [10] of PSR J0751+1807 in which the estimated mass with 1σ error bars is $2.1 \pm 0.2 M_{\odot}$. In addition, to 95% confidence, one of the two pulsars Ter 5 I and J has a reported mass larger than $1.68 M_{\odot}$ [11].

Whereas the observed simple mean mass of neutron stars with white dwarf companions exceeds those with neutron star companions by $0.25 M_{\odot}$, the weighted means of the two groups are virtually the same. The $2.1 M_{\odot}$ neutron star, PSR J0751+1807, is about 4σ from the canonical value of $1.4 M_{\odot}$. *It is furthermore the case that the 2σ errors of all but two systems extend into the range below $1.45 M_{\odot}$, so caution should be exercised before concluding that firm evidence of large neutron star masses exists.* Continued observations, which will reduce the observational errors, are necessary to clarify this situation.

Masses can also be estimated for another handful of binaries which contain an

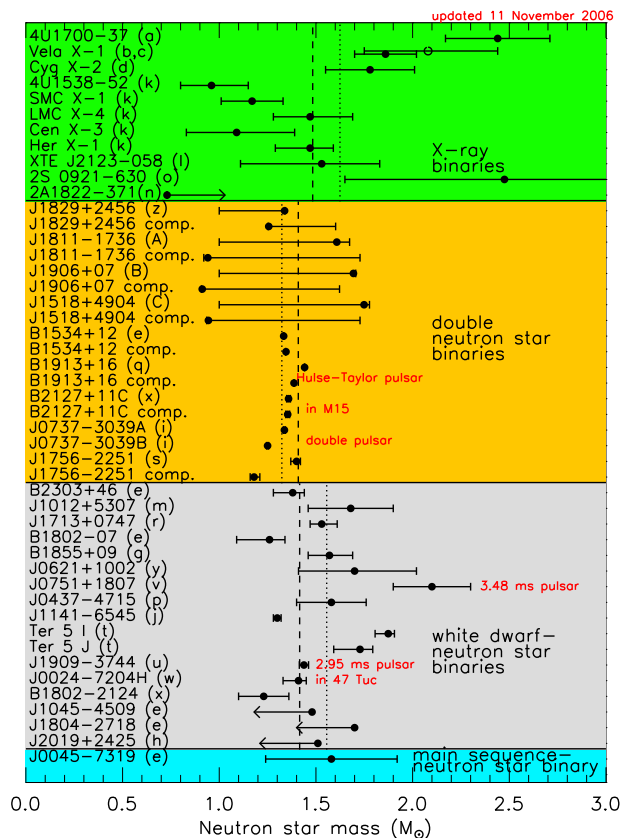


Figure 4. Measured and estimated masses of neutron stars in binarie pulsars (gold, silver and blue regions online) and in x-ray accreting binaries (green). For each region, simple averages are shown as dotted lines; error weighted averages are shown as dashed lines. For labels and other details, consult Ref. [8].

accreting neutron star emitting x-rays. Some of these systems are characterized by relatively large masses, but the estimated errors are also large. The system of Vela X-1 is noteworthy because its lower mass limit (1.6 to $1.7M_{\odot}$) is at least mildly constrained by geometry [12].

Raising the limit for the neutron star maximum mass could eliminate entire families of EOS's, especially those in which substantial softening begins around 2 to $3n_s$. This could be extremely significant, since exotica (hyperons, Bose condensates, or quarks) generally reduce the maximum mass appreciably.

Ultimate energy density of observable cold baryonic matter

Measurements of neutron star masses can set an upper limit to the maximum possible energy density in *any* compact object. It has been found [13] that no causal EOS has a central density, for a given mass, greater than that for the Tolman VII [14] analytic solution. This solution corresponds to a quadratic mass-energy density ρ dependence

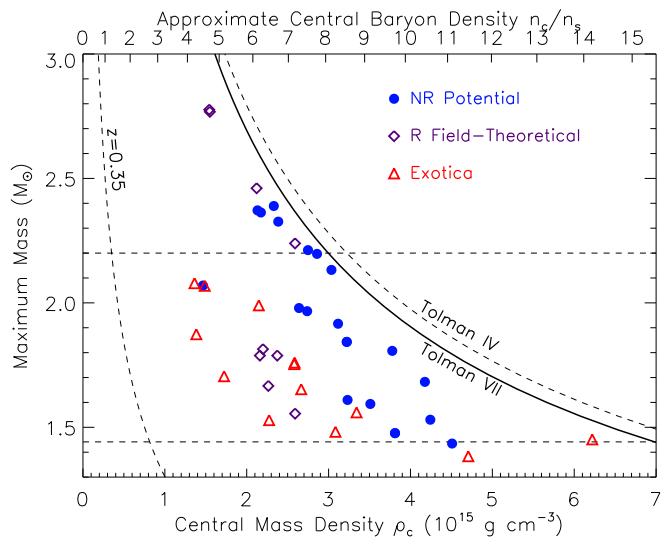


Figure 5. Model predictions are compared with results from the Tolman IV and VII analytic solutions of general relativistic structure equations. NR refers to non-relativistic potential models, R are field-theoretical models, and Exotica refers to NR or R models in which strong softening occurs, due to hyperons, a Bose condensate, or quark matter as well as self-bound strange quark matter. Constraints from a possible redshift measurement of $z = 0.35$ is also shown. The dashed lines for 1.44 and 2.2 M_{\odot} serve to guide the eye. Figure taken from Ref. [13].

on r , $\rho = \rho_c[1 - (r/R)^2]$, where the central density is ρ_c . For this solution,

$$\rho_{c,T VII} = 2.5\rho_{c,Inc} \simeq 1.5 \times 10^{16} \left(\frac{M_{\odot}}{M}\right)^2 \text{ g cm}^{-3}. \quad (1)$$

A measured mass of 2.2 M_{\odot} would imply $\rho_{max} < 3.1 \times 10^{15} \text{ g cm}^{-3}$, or about $8n_s$.

Figure 5 displays maximum masses and accompanying central densities for a wide variety of neutron star EOS's, including models containing significant softening due to “exotica”, such as strange quark matter. The upper limit to the density could be lowered if the causal constraint is not approached in practice. For example, at high densities in which quark asymptotic freedom is realized, the sound speed is limited to $c/\sqrt{3}$. Using this as a strict limit at all densities, the Rhoades & Ruffini [15] mass limit is reduced by approximately $1/\sqrt{3}$ and the compactness limit $GM/Rc^2 = 1/2.94$ is reduced by a factor $3^{-1/4}$ to $1/3.8$ [16]. In this extreme case, the maximum density would be reduced by a factor of $3^{-1/4}$ from that of Eq. (1). A 2.2 M_{\odot} measured mass would imply a maximum density of about $4.2n_s$.

5. Gravitational wave signals during mergers of binary stars

Mergers of compact objects in binary systems, such as a pair of neutron stars (NS-NS), a neutron star and a black hole (NS-BH), or two black holes (BH-BH), are expected to be prominent sources of gravitational radiation [17]. The gravitational-wave signature of such systems is primarily determined by the chirp mass $M_{chirp} =$

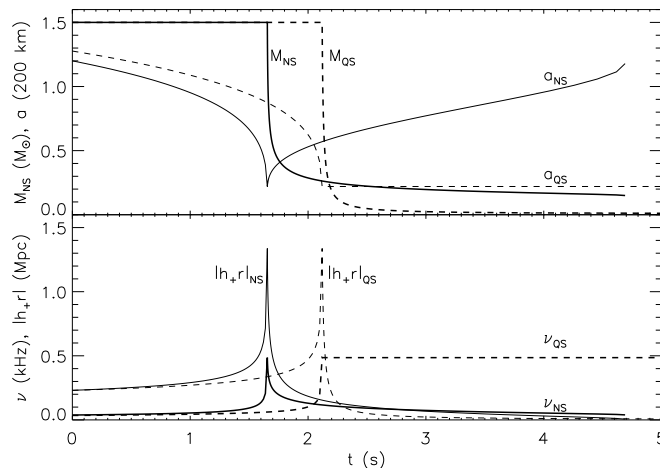


Figure 6. Physical and observational variables in mergers between low-mass black holes and neutron stars or self-bound quark stars. The total system mass is $6 M_{\odot}$ and the initial mass ratio is $q = 1/3$ in both cases. The initial radii of the neutron star and quark star were assumed to be equal. The time scales have arbitrary zero points. Upper panel displays semi-major axis a (thick lines) and component mass M_{NS}, M_{QS} (thin lines) evolution. Lower panel displays orbital frequency ν (thick lines) and strain amplitude $|h_+ r|$ evolution. Solid curves refer to the neutron star simulation and dashed curves to the quark star simulations. Figure taken from Ref. [8].

$(M_1 M_2)^{3/5} (M_1 + M_2)^{-1/5}$, where M_1 and M_2 are the masses of the coalescing objects. The radiation of gravitational waves removes energy which causes the mutual orbits to decay. For example, the binary pulsar PSR B1913+16 has a merger timescale of about 250 million years, and the pulsar binary PSR J0737-3039 has a merger timescale of about 85 million years [18], so there is ample reason to expect that many such decaying compact binaries exist in the Galaxy. Besides emitting copious amounts of gravitational radiation, binary mergers have been proposed as a source of the r-process elements [19] and the origin of the shorter-duration gamma ray bursters [20].

Observations of gravity waves from merger events can simultaneously measure masses and radii of neutron stars, and could set firm limits on the neutron star maximum mass [21, 22]. Binary mergers for the two cases of a black hole and a normal neutron star and a black hole and a self-bound strange quark matter star (Fig. 6) illustrate the unique opportunity afforded by gravitational wave detectors due to begin operation over the next decade, including LIGO, VIRGO, GEO600, and TAMA.

A careful analysis of the gravitational waveform during inspiral yields values for not only the chirp mass M_{chirp} , but for also the reduced mass $M_{BH} M_{NS} / M$, so that both M_{BH} and M_{NS} can be found [23]. The onset of mass transfer can be determined by the peak in ω , and the value of ω there gives a . A general relativistic analysis of mass transfer conditions then allows the determination of the star's radius [22]. Thus a point on the mass-radius diagram can be estimated [24]. The combination $h_+ \omega^{-1/3}$ depends only on a function of q , so the ratio of that combination and knowledge of q_i

should allow determination of q_f . From the Roche condition and knowledge of a_f from ω_f , another mass-radius combination can be found.

The sharp contrast between the evolutions during stable mass transfer of a normal neutron star and a strange quark star should make these cases distinguishable. For strange quark matter stars, the differences in the height of the frequency peak and the plateau in the frequency values at later times are related to the differences in radii of the stars at these two epochs. It could be an indirect indicator of the maximum mass of the star: the closer is the star's mass before mass transfer to the maximum mass, the greater is the difference between these frequency values, because the radius change will be larger. Together with radius information, the value of the maximum mass remains the most important unknown that could reveal the true equation of state at high densities.

Acknowledgments

This work was supported in part by the U.S. Department of Energy under the grant DOE/DE-FG02-93ER40756.

References

- [1] Collins J C and Perry M J 1975 *Phys. Rev. Lett.* 30, 1353
- [2] Pons J A, Steiner A W, Prakash M and Lattimer J A 2001 *Phys. Rev. Lett.* 86, 5223
- [3] Ellis P J, Lattimer J M and Prakash M 1996 *Comments in Nuclear and Particle Physics* 22, 63
- [4] Lattimer J M, Pethick C J, Prakash M and Haensel P, 1991, *Phys. Rev. Lett.* 66, 2701
- [5] Page D, Prakash M, Lattimer J M, and Steiner A W, 2000 *Phys. Rev. Lett.* 85, 2048
- [6] Page D, Lattimer J M, Prakash M and Steiner A W 2004 *Astrophys. Jl* 155, 623
- [7] Lattimer J M and Prakash M 2004 *Science* 304,536
- [8] Lattimer J M and Prakash M 2006, astro-ph/0612440
- [9] Bethe H A and Brown G E 1998 *Astrophys. Jl* 506, 780
- [10] Nice D J et al. 2005 *Astrophys. Jl.* 634, 1242
- [11] Ransom S M 2005 *Science* 307, 892
- [12] Quaintrell et al. 2003 *Astron. Astrophys.* 401, 303
- [13] Lattimer J M and Prakash M *Phys. Rev. Lett.* 94, 111101
- [14] Tolman R C 1939 *Phys. Rev.* 55, 364
- [15] Rhoades C E and Ruffini R 1974 *Phys. Rev. Lett.* 32, 324
- [16] Lattimer J M, Prakash M, Masak D, and Yahil A 1990 *Astrophys. Jl.* 355, 241
- [17] Thorne K S, 1973 *Three Hundred Years of Gravitation*, ed. S. W. Hawking and W. Israel, Cambridge Univ. Press, Cambridge, Ch. 9
- [18] Lyne A. G. et al., 2004 *Science* 303, 1153
- [19] Lattimer J M and Schramm D, 1976 *Astrophys. Jl.* 210, 549
- [20] Eichler D et al., 1989 *Science* 340, 126
- [21] Prakash M and Lattimer J M 2003, *J. Phys. G. Nucl. Part. Phys.* 30, S451
- [22] Ratkovic S, Prakash M and Lattimer J M 2005, astro-ph/0512136
- [23] Cutler C and Flanagan E E 1994, *Phys. Rev.* D49, 2658
- [24] Faber J A et al., 2002 *Phys. Rev. Lett.* 89, 231102